Membrane-Bound Conformation of Mastoparan-X, a G-Protein-Activating Peptide†

Kaori Wakamatsu,*,‡ Akihiko Okada,§ Tatsuo Miyazawa,∥ Masanao Ohya,‡ and Tsutomu Higashijima*,⊥

Faculty of Engineering, Gunma University, Kiryu, Gunma 376, Japan, Tsukuba Research Laboratory, Sumitomo Chemical Company, Ltd., Kitahara 6, Tsukuba, Ibaraki 300-32, Japan, Protein Engineering Research Institute, Furuedai, Suita, Osaka 565, Japan, and Department of Pharmacology, University of Texas Southwestern Medical Center at Dallas, 5323 Harry Hines Boulevard, Dallas, Texas 75235-9041

Received December 28, 1991; Revised Manuscript Received April 1, 1992

ABSTRACT: Mastoparan-X, a tetradecapeptide from wasp venom, has been proposed to cause secretion from various kinds of cells by the direct activation of GTP-binding regulatory proteins (G proteins) that couple to phospholipase C. The mechanism of the activation has been shown to be very similar to that of G-protein-coupled receptors in vitro, and the interaction with membranes seems to be very important for the activation of G proteins that are membrane-bound [Higashijima, T., Uzu, S., Nakajima, T., & Ross, E. M. (1988) *J. Biol. Chem. 263*, 6491–6494]. We report here the precise vesicle-bound conformation of mastoparan-X in the presence of perdeuterated phospholipid vesicles, determined by two-dimensional ^{1}H-NMR analyses of transferred nuclear Overhauser effects, combined with distance geometry and molecular dynamics calculations. Of 14 amino acid residues, the C-terminal 12 residues take an α-helical conformation upon binding to the phospholipid bilayer. The overall structure of the α-helix is amphiphilic, with three lysine side chains located on one side and with hydrophobic side chains on the other side. This conformation of mastoparan-X was maintained both in the gel and in the liquid-crystalline phases of the membranes. The conformation described herein will provide a useful basis for understanding conformation–activity relationships of mastoparan analogs as activators of G proteins. These studies will help to design novel potent analogs for the regulation of G proteins and to analyze receptor–G-protein interactions.

Mastoparans [reviewed by Nakajima et al. (1986)] are a group of toxic peptides found in venom sacs of wasps (Table I). They nonselectively stimulate exocytosis, including the release of histamine from mast cells (Hirai et al., 1979). They also show mitogenic activity for Swiss 3T3 cells in synergy with growth hormone (Gil et al., 1991). Many of these activities, including histamine release, are blocked by the pretreatment of these cells with pertussis toxin, which ADP-ribosylates G_i-type G proteins[1] and renders them insensitive to hormonal regulation [Higashijima et al., 1987; reviewed by Gilman (1987)]. These observations suggest that the target of mastoparan is widely expressed in many cells and that mastoparan acts on or before G proteins in signal transduction pathways.

We have recently shown that mastoparan in vitro activates purified G proteins (G_o and G_i) by accelerating the dissociation of G-protein-bound GDP more than 20-fold and that the ADP-ribosylation of these G proteins by pertussis toxin inhibits the effect of mastoparan on G proteins. Thus, the mechanism of the activation of G proteins by mastoparan seems to be very similar to that of G-protein-coupled receptors (Higashijima et al., 1988). These data support the hypothesis that mastoparan causes the direct activation of G proteins in those cells by bypassing receptors that couple to G proteins.

The binding of mastoparans to G protein, however, does not seem to be a simple process because G proteins are membrane-bound proteins that face the cytoplasmic side of the plasma membrane. Direct evidence of the membrane translocation of mastoparan has not been obtained yet, but the inside-negative membrane potential may be a major force for such translocation of model peptides (de Kroon et al., 1991a,b). Mastoparans have strong affinity for phospholipids. We have shown preliminarily that transferred NOE (TRNOE) analyses of mastoparan-X (MP-X) in the presence of perdeuterated dilauroylphosphatidylcholine vesicles can be used to analyze the membrane-bound conformation (Wakamatsu et al., 1983). These studies, combined with CD analyses, showed that mastoparan in aqueous solution takes an α-helical conformation in the presence of phospholipid bilayers or micelles although it does not adopt any definite conformation at low ionic strength in the absence of phospholipids (Higashijima et al., 1983, 1984). The fact that the addition of phospholipid membrane enhances the activation of G proteins by mastoparan suggests that the membrane-bound conformation of mastoparan is important for the efficient activation of G proteins (Higashijima et al., 1988, 1990).

The preliminary NMR and CD studies have not given a precise vesicle-bound conformation of mastoparan or a clear picture of its interaction with phospholipid vesicles. We have now analyzed the interaction of mastoparan with phospholipid

Table I: Primary Structure of Mastoparans

mastoparan (MP)	H-Ile-Asn-Leu-Lys-Ala-Leu-Ala-Ala-Leu-Ala-Lys-Lys-Ile-Leu-NH_2
mastoparan-X (MP-X)	H-Ile-Asn-Trp-Lys-Gly-Ile-Ala-Ala-Met-Ala-Lys-Lys-Leu-Leu-NH_2

† These studies were supported by the International Scientific Research Program (Joint Research) (K.W. and T.H.), by a grant-in-aid from the Ministry of Education, Science and Culture, Japan, by a grant from the Asahi Glass Foundation (K.W.), and by U.S. Public Health Service Grant GM40676 (T.H.).

‡ Gunma University.
§ Sumitomo Chemical Co., Ltd.
∥ Protein Engineering Research Institute.
⊥ University of Texas Southwestern Medical Center at Dallas.

[1] Abbreviations: CD, circular dichroism; NMR, nuclear magnetic resonance; NOE, nuclear Overhauser effect; TRNOE, transferred NOE; NOESY, NOE spectroscopy; ROESY, rotating-frame NOE spectroscopy; TOCSY, total correlation spectroscopy; G protein, GTP-binding regulatory protein; MP, mastoparan; MP-X, mastoparan-X; DPPC-d_{80}, perdeuterated dipalmitoylglycerophosphocholine; rms, root mean square; MW, molecular weight; TRNOESY, transferred NOESY.

0006-2960/92/0431-5654$03.00/0

bilayers closely in H_2O solution by analyses of TRNOESY spectra of MP-X in the presence of perdeuterated lipid vesicles. The distance constraints derived from TRNOE data were then used in distance geometry calculation to generate structures that fit both to NMR data and to fixed bond lengths and bond angles. Because these structures are usually trapped in local subminima and show large rms differences among them, they were refined by restrained molecular dynamics calculation to reach global minima. Here we report the precise vesicle-bound conformation of MP-X, a mastoparan from *Vespa xanthoptera* that shows activities very similar to those of mastoparan both in vivo and in vitro (Higashijima et al., 1990).

Experimental Procedures

Preparation of NMR Samples. MP-X was purchased from Peninsula (Belmont, CA). Synthesis of perdeuterated L-α-dipalmitoylglycerophosphocholine (DPPC-d_{80}) has been reported elsewhere (Kingsley & Feigenson, 1979; Wakamatsu et al., 1986a). Small unilamellar vesicles were prepared as reported previously (Wakamatsu et al., 1983, 1986a) with minor modifications. Briefly, a thin film of DPPC-d_{80}, formed by evaporation of chloroform solution, was sonicated in the presence of D_2O at 20 W for 20 min (probe type), and the precipitate was removed by centrifugation at 1000g for 10 min. Electron microscopy of DPPC vesicles prepared similarly showed that the diameter is 200–300 Å. Multilamellar vesicles of DPPC-d_{80} were also prepared by sonication with a bath-type sonicator. Lipid concentration was determined according to the method of Bartlett (1959).

NMR Measurements. Proton NMR spectra were recorded on Bruker AM-400 and AMX-600 spectrometers operating at 400 and 600 MHz, respectively. The chemical shifts were measured relative to the methyl resonance of 4,4-dimethyl-4-silapentane-1-sulfonate, used as an internal reference. Peptide was dissolved in 90% H_2O/10% D_2O or 99.98% D_2O. Sample pH (direct pH meter reading) was adjusted to 3.5. We used a new type of microtube that enabled us to reduce the sample volume to 0.2 mL without sacrificing resolution (Shigemi, Tokyo) (Takahashi & Nagayama, 1988). The temperature was kept at 45 °C unless otherwise specified. Since the phase transition temperature of DPPC-d_{80} is 35.5 °C, the vesicles are in the liquid-crystalline phase at 45 °C (Wakamatsu et al., 1986a). Measurements of TRNOE's in the presence of gel-phase vesicles were performed at 30 °C.

Two-dimensional TOCSY (Bax & Davies, 1985) and NOESY (Jeener et al., 1979; Macura et al., 1981) spectra were measured on an 8 mM MP-X sample in the presence of 2 mM DPPC-d_{80} in the phase-sensitive mode using the time-proportional phase increment (Bodenhausen et al., 1984). CD study showed that the formation of helical structure by the addition of vesicles was saturated by 80 molar excess of PC, suggesting that 25 μM (of 4 mM) MP binds to 2 mM DPPC-d_{80}; 25 μM is only 0.31% of total MP, but this is enough to detect TRNOE when bound MP-X is in fast exchange (exchange rate >10 s^{-1}) with free MP-X (Clore & Gronenborn, 1982). For samples that contained 90% H_2O/10% D_2O, the water resonance was eliminated by the jump-and-return read pulse (Plateau & Gueron, 1982) for NOESY and by presaturation for TOCSY. The mixing times were 300 ms for NOESY and 50 ms for TOCSY. In preliminary one-dimensional NOE experiments, spin-diffusion effects (Kalk & Berendsen, 1976) were not observed with irradiations of up to 0.5 s duration (Wakamatsu et al., 1983; confirmed in this work). A total of 512 measurements with increasing t_1 values were made, and 64 transients were accumulated for each measurement. For measurements at 400 and 600 MHz, 2048 or 4096 data points for t_2 were taken, and the spectral widths along f_2 were 5000 and 8000 Hz, respectively. The time-domain data were multiplied by squared cosine bell functions in both dimensions and expanded by zero-filling to give 2048 × 1024 (400 MHz) and 4096 × 2048 (600 MHz) frequency-domain data after Fourier transformation.

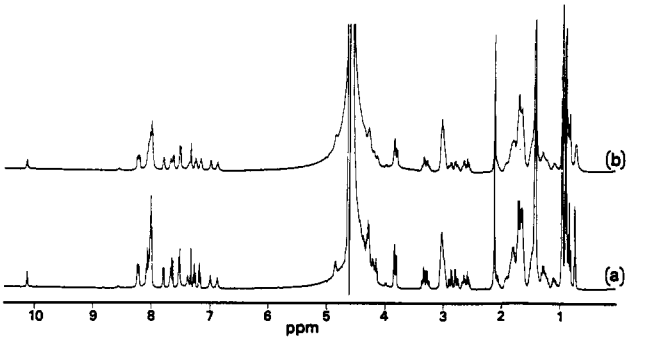

FIGURE 1: 400-MHz proton NMR spectrum of MP-X (4 mM) in 90% H_2O/10% D_2O (a) in the absence and (b) in the presence of DPPC-d_{80} vesicles (2 mM) at pH 3.5 and 45 °C.

Computation Procedure. For the determination of structure, variable target-function distance-geometry calculations in dihedral angle space (Braun & Go, 1985) were carried out using the program DADAS. In DADAS calculations, upper limits on the interproton distances of 2.7, 3.3, and 4.0 Å were used for strong, medium, and weak NOE peaks, respectively. Similar values have been used for small proteins and peptides (Clore et al., 1986). The basis of the choice of these values is empirical, and as such, these values might not be best to represent NOE intensities for a peptide bound to large vesicles. Nevertheless, the choice of these values was supported as follows. We chose the Trp C_4H–C_5H cross-peak (2.5 Å) as a reference standard (4–5 levels in the contour plot drawn by an intensity interval of 2^n, where n is the level number). This was chosen because geminal protons normally used as a reference were overlapped or too broad. NOEs were classified as strong, medium, and weak for $n > 4$, $4 > n > 2$, and $2 > n > 1$, respectively. N_iH–$N_{i+1}H$ (2.8 Å) and α_iH–$N_{i+1}H$ (3.5 Å) pairs in α-helical structure would be 50% (3–4 levels in the contour plot, medium) and 13% (1–2 levels, weak) of the reference standard. The intensities of many peaks are consistent with the criteria (Figure 3). For NOEs involving methyl groups of alanine and isoleucine, a pseudoatom was introduced at the center of mass of the three methyl protons, and the distance correction was made by adding 1.5 Å to the upper limit (Wüthrich et al., 1983). Distance constraints for Cδ methyl protons of leucine, for which stereospecific assignment could not be made, were replaced by a pseudoatom placed at the center of mass of the six methyl protons, and a distance correction term of 2.0 Å was added to the upper limit value. Because this version of DADAS does not permit the placement of a pseudoatom at the center of mass of the glycine Cα methylene protons, distance constraints involving the two equivalent Hα methylene protons of Gly^5 were replaced by the Cα atom, and a distance correction term of 1.0 Å was added to the upper limit. For other methylene protons that could not be assigned stereospecifically, pseudoatoms located at the center of mass of the methylene protons were used, and the distance correction term of 1.0 Å was added to the upper limit. DADAS calculations were executed on a VAX 8530 computer with 53 interresidue and 16 intraresidue NOE constraints. From 20 random structures, 13 structures with the maximum distance violation of less than 0.5 Å were selected.

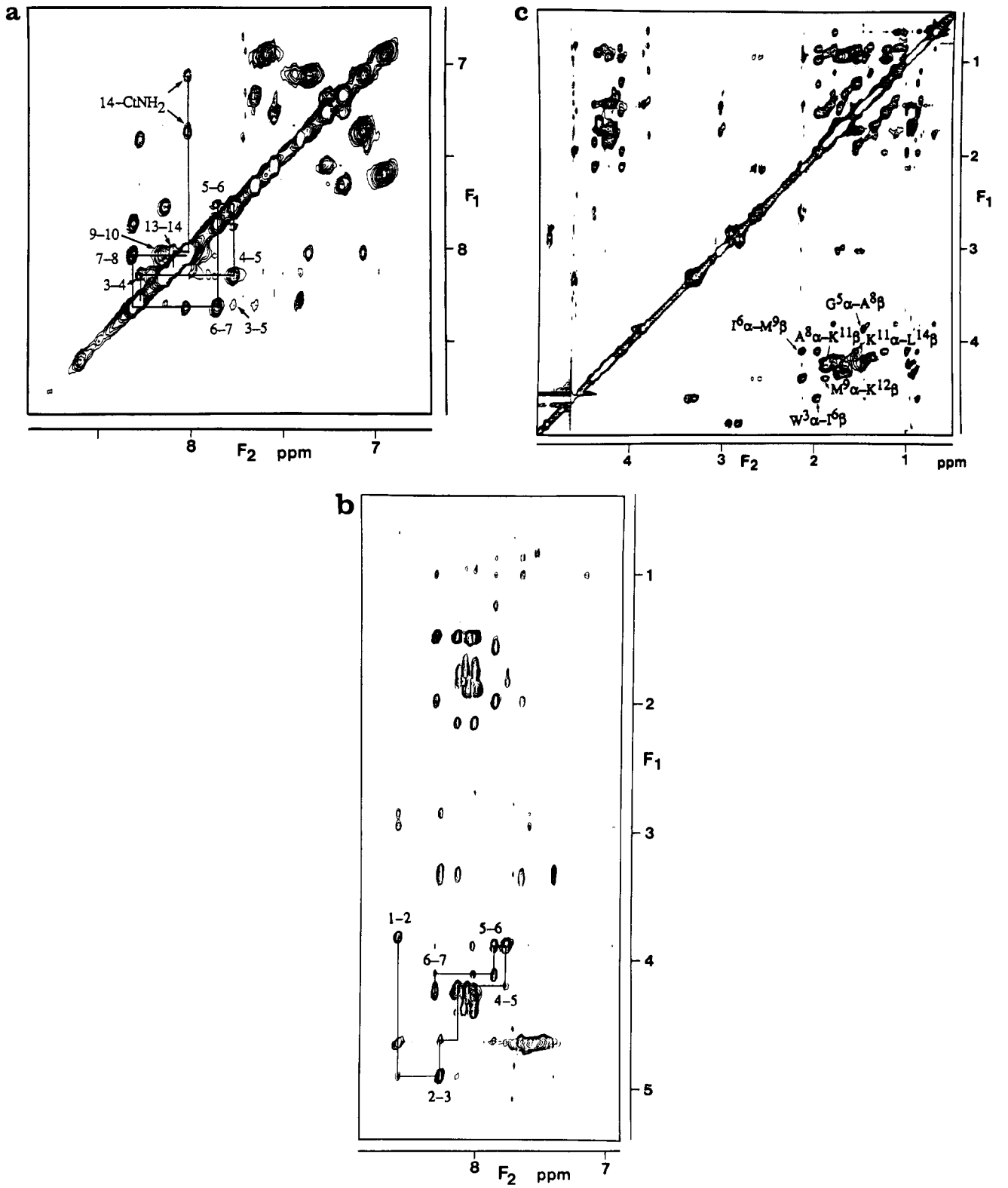

FIGURE 2: 400-MHz TRNOESY spectra of MP-X (8 mM) in 90% H_2O/10% D_2O in the presence of DPPC-d_{80} (2 mM) at 45 °C. (a) NH/NH region; (b) aliphatic/NH region; (c) aliphatic/aliphatic region. The mixing time is 300 ms. In (a) and (b), each sequential NOE peak is marked with the residue number pair.

These 13 structures were then refined with restrained molecular dynamics calculations using the program XPLOR, run on a silicon graphics IRIS 4D80GTB computer (Brünger et al., 1987). Electrostatic interaction was neglected in this calculation, and a repel energy function was used for van der Waals potentials (Kraulis et al., 1989). The distance constraint for the interproton distance was set to 1.8–2.7, 1.8–3.3, and 1.8–4.0 Å for strong, medium, and weak NOE data, respectively. The $(\langle r^{-6}\rangle)^{-1/6}$ distance averaging method was used for equivalent protons. For distance constraints that involved nonequivalent protons that could not be stereospecifically assigned, the program adopted center-average distances that are similar to the pseudoatom representation. The NOE pseudopotential was described by the square-well function, and the force constant was set to 50 kcal·mol^{-1}·Å^{-2}. The force constants of bonds, angles, and improper torsions were set to

Table II: Proton Chemical Shifts (ppm) of Mastoparan-X in H_2O Solution at pH 3.5 and 45 °C

residue	NH	α	β	others
Ile[1]		3.81	1.78	γ_2 1.39, 1.11; γ_3 0.69; δ_3 0.85
Asn[2]	8.61	4.89	2.91, 2.83	NH 7.60, 6.95
Trp[3]	8.28	4.62	3.35, 3.20	C2 7.40, C4 7.64, C5 7.17, C6 7.26, C7 7.54
Lys[4]	8.13	4.20	1.83, 1.76	γ_2 1.33, δ_2 1.70, ϵ_2 3.01
Gly[5]	7.76	3.87		
Ile[6]	7.86	4.12	1.97	γ_2 1.54, 1.23; γ_3 0.98; δ_3 0.87
Ala[7]	8.31	4.26	1.48	
Ala[8]	8.03	4.25	1.47	
Met[9]	8.02	4.41	2.14, 2.14	γ_2 2.67, 2.59; ϵ_3 2.13
Ala[10]	8.16	4.27	1.49	
Lys[11]	8.07	4.25	1.88, 1.81	γ_2 1.52, 1.46; δ_2 1.75; ϵ_2 3.03
Lys[12]	8.01	4.30	1.86, 1.86	γ_2 1.52, 1.46; δ_2 1.75; ϵ_2 3.04
Leu[13]	8.10	4.38	1.72, 1.72	γ 1.69; δ_3 0.97, 0.92
Leu[14]	8.02	4.35	1.74, 1.74	γ 1.69; δ_3 0.98, 0.93
NH_2	7.36, 7.06			

1000 kcal·mol^{-1}·Å^{-2}, 500 kcal·mol^{-1}·rad^{-2}, and 500 kcal·mol^{-1}·rad^{-2}, respectively. The improper torsion potential keeps the planarity of trans-peptide bonds and aromatic rings. The XPLOR calculation was performed in two stages. The first stage was 2 ps of high-temperature (2000 K) dynamics to correct residual distance violation, and the second stage was cooling for final refinement. The temperature was decreased to 300 K in 50 K steps during the second stage. Each structure was then energy-minimized with NOE constraints. Nine XPLOR structures that had no distance violation larger than 0.3 Å were finally selected out of the initial group of 13 DADAS structures.

Results

Spectral Change of MP-X upon Addition of the DPPC-d_{80} Bilayer. Figure 1a,b shows 400-MHz ^{1}H-NMR spectra of 4 mM MP-X in 90% H_2O/10% D_2O in the absence and presence of 1 mM DPPC-d_{80} vesicles at 45 °C. Upon addition of the vesicles, peptide resonances were uniformly broadened, reflecting the exchange of MP-X between the free state and the vesicle-bound state. Changes in the chemical shift of each signal were not observed, but peptide resonances were broadened with increasing temperature (data not shown). These observations show that the two states are actually in slow exchange at 45 °C.

Transferred NOE (TRNOE). Because MP-X is a medium-sized (MW = 1700), flexible molecule, it did not show any NOE at 45 °C in the absence of vesicles (data not shown). In the presence of vesicles, however, many strong NOESY peaks are observed because of the transfer of strong negative NOE's in the vesicle-bound state to the free state (Figure 2). These are TRNOE's which reflect the conformation of peptide in the vesicle-bound state but not the conformation in the free state (Wakamatsu et al., 1983). These TRNOE data can be interpreted as are conventional NOE data for larger proteins (Albrand et al., 1979; Clore & Gronenborn, 1982). An indistinguishable NOE pattern was obtained with multilamellar vesicles, though absolute intensities of NOEs might be slightly weaker than in the case of small unilamellar vesicles.

Resonance Assignments of MP-X. Sequence-specific resonance assignments were performed using TOCSY (Wüthrich, 1986; data not shown) and NOESY (Figure 2a,b) data in the presence of vesicles. Trp[3], Gly[5], and Met[9] were used as starting points for this purpose. Chemical shifts obtained by the analyses are listed in Table II. These sequential assignments were confirmed by ROESY measurements in the absence of vesicles (not shown).

Cβ protons of Trp[3] were assigned on the basis of a study on stereospecifically deuterated Trp in small flexible peptides:

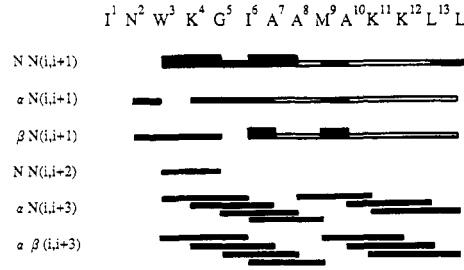

FIGURE 3: Summary of sequential and medium-range NOE's. NOE connectivities of specified proton pairs that were observed in the spectrum are marked with black bars. Thick and thin bars show the NOE is medium and weak, respectively. NOE connectivities that may exist but cannot be observable due to resonance overlapping are marked with open bars.

the *pro-S* (Hβ3) and *pro-R* (Hβ2) β protons of the Trp residue in these peptides in aqueous solution appeared at lower and higher field, respectively (Kobayashi et al., 1984). We first assumed that the two Cβ protons of Trp[3] in MP-X appear in the same order because the MP-X molecule is flexible and does not take an ordered conformation in aqueous solution. Structure calculations with intraresidual NOE constraints using this assumption resulted in the side chain conformation with the χ_1 angle (the dihedral angle defined by N_α–C_α–C_β–C3) of about −60° and the χ_2 angle (the dihedral angle defined by C_α–C_β–C3–C2) of about +90°. This side chain conformation of Trp predominates both for zwitterionic tryptophan in aqueous solution and for Trp residues in proteins (O. Koshio, M. Tasumi, and T. Miyazawa, unpublished results).

Effect of Phospholipid Phase on Interaction with MP-X. The TRNOE spectrum of MP-X was also measured at 30 °C, at which the DPPC-d_{80} membrane is in the gel phase (the phase transition temperature is 35.5 °C). Almost all NOE cross-peaks [NN(i,i+1), αN(i,i+3), and αβ(i,i+3) NOE's] observed at 45 °C were also detected at this temperature (data not shown). This observation indicates that the conformation of MP-X bound to a phosphatidylcholine bilayer is not affected by the phase of the membrane, either liquid-crystalline or gel.

Secondary Structure of Membrane-Bound MP-X. Sequential and medium-range NOE's are summarized in Figure 3. NOE patterns characteristic of an α-helical conformation (Wüthrich, 1986) are apparent from Trp[3] to C-terminal Leu[14] by sequential NN(i,i+1), αN(i,i+3), and αβ(i,i+3) NOE's. This was confirmed by computer calculation with distance geometry and molecular dynamics programs.

Calculated Structures. Figure 4a shows the superposition of nine structures calculated with XPLOR programs. Only backbone and Cβ atoms are shown. As expected from the NOE pattern shown in Figure 3, the peptide backbone from Trp[3] to Leu[13] is well converged and is in the α-helical conformation. On the other hand, the N-terminal two residues are in the extended conformation. Average rms differences of structures obtained after DADAS and XPLOR calculations were 1.7 ± 0.6 and 0.9 ± 0.4 Å, respectively, for backbone atoms (–N–C_α–CO–) and 3.0 ± 0.4 and 2.1 ± 0.3 Å, respectively, for all atoms, excluding residues 1, 2, and 14. Figure 4b shows the structure that has the least violation of the constraints in the restrained molecular dynamics calculation. Three lysine side chains are located on one side while hydrophobic side chains of Ile, Trp, Met, and Leu are located on the other side, making the structure amphiphilic as a whole.

Discussion

Interaction of MP-X with Lipid Vesicles. The TRNOE data presented here indicate that MP-X forms an amphiphilic

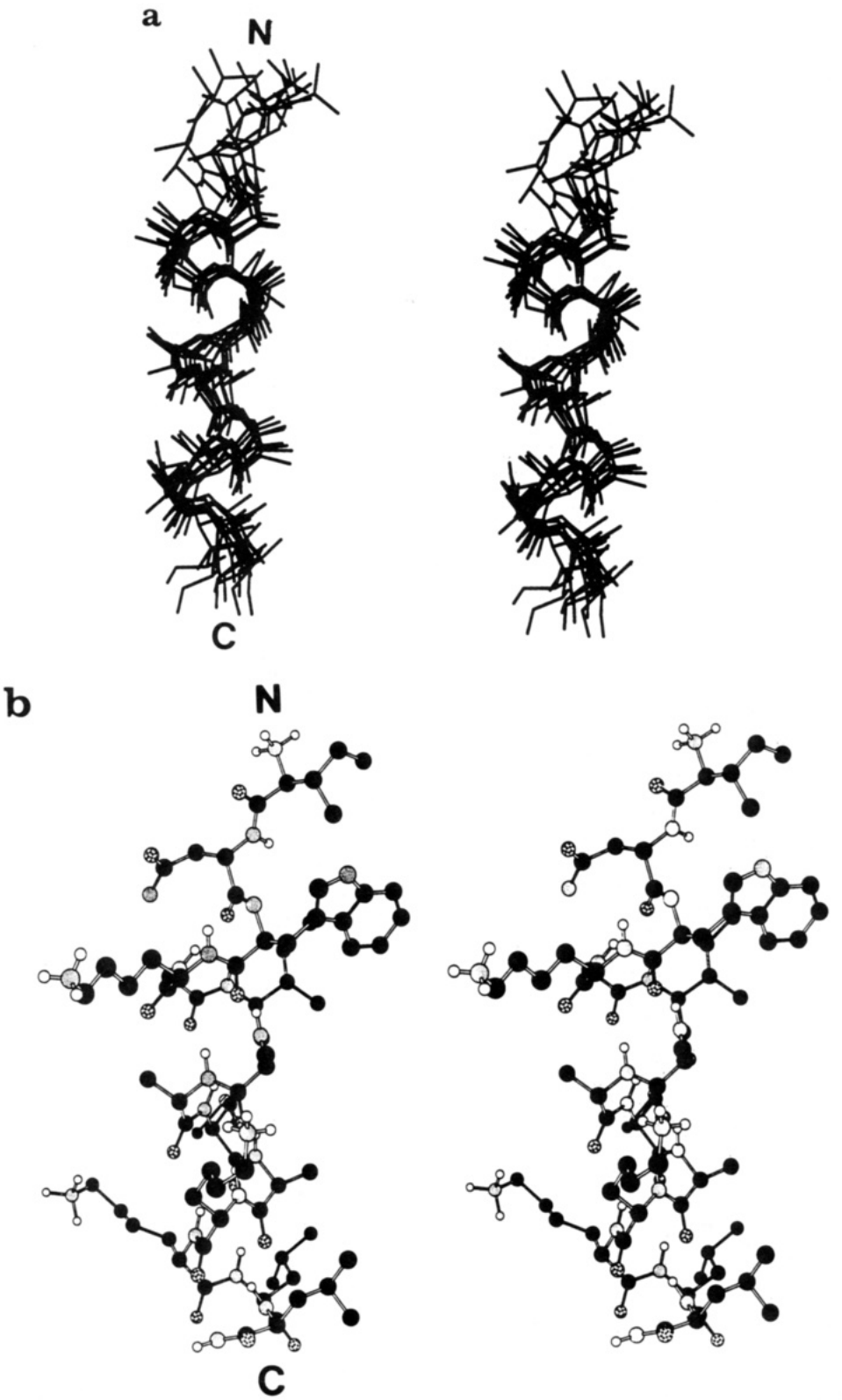

FIGURE 4: Conformation of membrane-bound MP-X (stereoview). (a) Superposition of nine calculated structures (only backbone and Cβ atoms are drawn); (b) structure with least violation.

helix when bound to phospholipid vesicles. The vesicle-bound conformation is unlikely to have been affected by the curvature of vesicles (diameter more than 200 Å), because MP-X is small compared to vesicles. Thus, MP-X as bound to a planar phospholipid surface is likely to have a similar conformation. This conformation presumably reflects the interaction of the hydrophobic face of the helix with the membrane bilayer and orientation of the positively charged face toward the aqueous medium. Both CD spectroscopy (Higashijima et al., 1983) of MP's and our preliminary one-dimensional TRNOE study (Wakamatsu et al., 1983) also suggested such a structure. However, CD spectroscopy neither allows determination of which residues are involved in formation of the helix nor provides any other absolute structural information. The one-dimensional TRNOE data also indicated helical structure, but detailed analysis was limited by signal overlaps and a lack of information on NH protons that was caused by H–D exchange.

By observing MP-X in H_2O using two-dimensional NMR, we have now succeeded in elucidating in detail the interaction of MP-X with phosphatidylcholine vesicles by the combined application of distance geometry and molecular dynamics to the TRNOE data. The proposed structure is a conservative interpretation of the data because possible structures were selected on the basis only of NOE data and of intramolecular constraints of bond lengths, bond angles, and steric hindrance. We made no assumptions about interactions with solvents, which include water, the hydrophobic interior of lipid, and the lipid head group.

The present study demonstrates that residues from Trp^3 to the C-terminal Leu^{14}-NH_2, but not the N-terminal two residues, take an α-helical conformation in the presence of DPPC-d_{80}. The α-helical structure in the Trp^3–Leu^{14} portion results in segregation of hydrophilic (three Lys) and hydrophobic (Trp, Ile, Met, and two Leu) side chains, providing the membrane-bound molecule with an amphiphilic character, a feature commonly found in lipoproteins, in lipid bilayers, and in many protein–protein interactions including the regulation of calmodulin (Segrest et al., 1973; Cox et al., 1985). If the Ile^1 residue was also involved in the α-helix, its hydrophobic side chain would be located on the hydrophilic side.

Mastoparans are known to self-aggregate at high peptide concentration and/or at high ionic strength (Higashijima et al., 1984). However, negative NOE's observed for MP-X in the presence of DPPC-d_{80} vesicles do not originate from a molecule in aggregated form. This is supported as follows. (1) Any salts were not added for the present experiments. (2) The chemical shifts of proton resonances did not change upon the addition of DPPC-d_{80} vesicles. Such clear shifts were observed for the aggregation of MP [Figure 1, compare with Figure 4 of Higashijima et al. (1984)]. (3) All the NOE peaks observed can be explained without assuming any peptide aggregation. These arguments support that negative NOE's are from TRNOE, which reflects the lipid-bound conformation of MP-X.

Relation of Membrane-Bound Conformation to Biological Activity. Schwyzer et al. have proposed that the physiological activities of many peptides are correlated with their affinities for the phospholipid membrane (Gysin & Schwyzer, 1983; Schwyzer, 1987). The structure–activity relationships of many peptides can be explained by their conformations in the membrane-bound state rather than in aqueous media (Higashijima et al., 1983; Wakamatsu et al., 1986a,b, 1987; Jelicks et al., 1989; Milon et al., 1990). These observations suggest the following scheme for peptide–receptor interaction: peptide molecules in the aqueous phase first bind to the lipid phase of plasma membranes of target cells and take some ordered conformation, which then migrate within the membrane to bind to the receptor molecule with a conformation similar to that in the lipid environment.

Activation of G protein by mastoparan is much more prominent when G proteins are reconstituted in lipid vesicles than when activation is measured in detergent (Lubrol) solution (Higashijima et al., 1988). The greater activation in the presence of phospholipids is probably due to a combination of the following effects: (1) appropriate active conformation of the mastoparan molecule as bound to the bilayer; (2) appropriate relative orientation of mastoparan and G-protein molecules in the membrane-bound state; and (3) increase of the effective concentration of mastoparan at the membrane surface, the location of the G protein. The active conformation of mastoparan seems to be very similar to that determined in this study. We have no data that indicate that the membrane-bound conformation of mastoparan is different from that of the micelle-bound form. However, the difference between the membrane- and micelle-bound conformations is suggested for melittin, an analogous peptide from honey bee venom (Wakamatsu et al., 1986b).[2]

Similarities between Mastoparans and G-Protein-Coupled Receptors. Studies of site-directed mutagenesis and chimeric G-protein-coupled receptors have suggested that the cationic N-terminal and C-terminal parts of the third inner loop and the N-terminal part of the C-terminal tail as well as a second inner loop are all important for the activation of G proteins and/or selectivity among G proteins (Kobilka et al., 1988; Lefkowitz & Caron, 1988; Ross, 1989). These sequences have been proposed to have amphiphilic properties, consistent with the structure determined for membrane-bound mastoparan in the present study (Ross, 1989).

In fact, mastoparan activates G proteins (G_o, G_i) by a mechanism similar to that of liganded receptors. Effects of mastoparan on G_i and G_o were inhibited by prior treatment of these G proteins by pertussis toxin. The effects are large for G_o and G_i, but not for G_t or G_s, showing clear selectivities among G proteins. Mastoparan does not require a high concentration of Mg^{2+} to promote the dissociation of GDP from G proteins. All of these characteristics hold for receptor-mediated activation of G proteins (Higashijima et al., 1988, 1990). In fact, mastoparan inhibited the ability of G_o proteins to increase the affinity of agonist binding to m2 muscarinic cholinergic receptor. These data support the idea that mastoparan binds to the receptor binding domain on G proteins (Higashijima et al., 1988, 1990).

These similarities suggest that mastoparan may be an excellent low molecular weight model for G protein binding domains of receptors. The membrane-bound conformation of mastoparan, rather than that in aqueous solution, should be a better approximation of its active conformation and, therefore, the conformation of the receptor's regulatory domain. The analysis of the G-protein-bound conformation of mastoparan analogs is now in progress. These studies will be useful for designing peptides that selectively activate different kinds of G proteins and, eventually, for understanding the specificity and generality of receptor–G-protein interaction.

Acknowledgments

We are grateful to Dr. S. Yokoyama and Dr. Y. Muto of the University of Tokyo for the use of a Bruker AM-400 spectrometer. We thank Dr. E. M. Ross of the University of Texas Southwestern Medical Center for his critical reading of the manuscript.

References

Albrand, J. P., Birdsall, B., Feeney, J., Roberts, G. C. K., & Burgen, A. S. V. (1979) *Int. J. Biol. Macromol. 1*, 37–41.

Bartlett, G. R. (1959) *J. Biol. Chem. 234*, 466–468.

Bax, A., & Davies, D. G. (1985) *J. Magn. Reson. 65*, 393–402.

Bodenhausen, G., Kogler, H., & Ernst, R. R. (1984) *J. Magn. Reson. 58*, 370–388.

Braun, W., & Go, N. (1985) *J. Mol. Biol. 186*, 611–626.

Brünger, A. T., Kuriyan, J., & Karplus, M. (1987) *Science 235*, 458–460.

Clore, G. M., & Gronenborn, A. M. (1982) *J. Magn. Reson. 48*, 402–417.

Clore, G. M., Nilges, M., Sukumaran, D. K., Brünger, A. T., Karplus, M., & Gronenborn, A. M. (1986) *EMBO J. 5*, 2729–2735.

[2] A. Okada, K. Wakamatsu, T. Higashijima, and T. Miyazawa, unpublished results.

Cox, J. A., Comte, M., Fitton, J. E., & DeGrado, W. F. (1985) *J. Biol. Chem. 260*, 2527–2534.
de Kroon, A. I. P. M., Vogt, B., van't Hof, R., de Kruijff, B. & de Gier, J. (1991a) *Biophys. J. 60*, 525–537.
de Kroon, A. I. P. M., de Gier, J., & de Kruijff, B. (1991b) *Biochim. Biophys. Acta 1068*, 111–124.
Gil, J., Higgins, T., & Rozengurt, E. (1991) *J. Cell Biol. 113*, 943–950.
Gilman, A. G. (1987) *Annu. Rev. Biochem. 56*, 615–649.
Gysin, B., & Schwyzer, R. (1983) *FEBS Lett. 158*, 12–16.
Higashijima, T., Wakamatsu, K., Takemitsu, M., Fujino, M., Nakajima, T., & Miyazawa, T. (1983) *FEBS Lett. 152*, 227–230.
Higashijima, T., Wakamatsu, K., Saito, K., Fujino, M., Nakajima, T., & Miyazawa, T. (1984) *Biochim. Biophys. Acta 802*, 157–161.
Higashijima, T., Uzu, S., Nakajima, T., & Miyazawa, T. (1987) in *Peptide Chemistry 1986* (Miyazawa, T., Ed.) pp 75–78, Protein Research Foundation, Osaka, Japan.
Higashijima, T., Uzu, S., Nakajima, T., & Ross, E. M. (1988) *J. Biol. Chem. 263*, 6491–6494.
Higashijima, T., Burnier, J., & Ross, E. M. (1990) *J. Biol. Chem. 265*, 14176–14186.
Hirai, Y., Yasuhara, T., Yoshida, H., Nakajima, T., Fujino, M., & Kitada, C. (1979) *Chem. Pharm. Bull. (Tokyo) 27*, 1942–1944.
Jeener, J., Meier, B. H., Bachman, P., & Ernst, R. R. (1979) *J. Chem. Phys. 71*, 4546–4553.
Jelicks, L. A., Broido, M. S., Becker, J. M., & Naider, F. R. (1989) *Biochemistry 28*, 4233–4240.
Kalk, A., & Berendsen, H. J. C. (1976) *J. Magn. Reson. 24*, 343–366.
Kingsley, P. B., & Feigenson, G. W. (1979) *Chem. Phys. Lipids 24*, 135–147.
Kobayashi, J., Higashijima, T., & Miyazawa, M. (1984) *Int. J. Pept. Protein Res. 24*, 40–47.
Kobilka, B. K., Kobilka, T. S., Daniel, K., Regan, J. W., Caron, M. G., & Lefkowitz, R. J. (1988) *Science 240*, 1310–1316.
Kraulis, P. J., Clore, G. M., Nilges, M., Jones, T. A., Pettersson, G., Knowles, J., & Gronenborn, A. M. (1989) *Biochemistry 28*, 7241–7257.
Lefkowitz, R. J., & Caron, M. G. (1988) *J. Biol. Chem. 263*, 4993–4996.
Macura, S., Hyang, Y., Suter, D., & Ernst, R. R. (1981) *J. Magn. Reson. 43*, 259–281.
Milon, A., Miyazawa, T., & Higashijima, T. (1990) *Biochemistry 29*, 65–75.
Nakajima, T., Uzu, S., Wakamatsu, K., Saito, K., Miyazawa, T., Yasuhara, T., Tsukamoto, Y., & Fujino, M. (1986) *Biopolymers 25*, S115–S121.
Plateau, P., & Gueron, M. (1982) *J. Am. Chem. Soc. 104*, 7310–7311.
Ross, E. M. (1989) *Neuron 3*, 141–152.
Schwyzer, R. (1987) in *Peptides 1986* (Theodoropoulos, D., Ed.) pp 7–23, Walter de Gruyter, Berlin.
Segrest, J. P., Jackson, R. L., Morrisett, J. D., & Gotto, A. M. (1973) *FEBS Lett. 38*, 247–253.
Takahashi, S., & Nagayama, K. (1988) *J. Magn. Reson. 76*, 347–351.
Wakamatsu, K., Higashijima, T., Fujino, M., Nakajima, T., & Miyazawa, T. (1983) *FEBS Lett. 162*, 123–126.
Wakamatsu, K., Okada, A., Suzuki, M., Higashijima, T., Masui, Y., Sakakibara, S., & Miyazawa, T. (1986a) *Eur. J. Biochem. 154*, 607–615.
Wakamatsu, K., Okada, A., Higashijima, T., & Miyazawa, T. (1986b) *Biopolymers 25*, S193–200.
Wakamatsu, K., Okada, A., Miyazawa, T., Masui, Y., Sakakibara, S., & Higashijima, T. (1987) *Eur. J. Biochem. 163*, 331–338.
Wüthrich, K. (1986) *NMR of Proteins and Nucleic Acids*, Wiley, New York.
Wüthrich, K., Billeter, M., & Braun, W. (1983) *J. Mol. Biol. 169*, 949–961.